

# Non-canonical two-field inflation to order $\xi^2$

Yun-Chao Wang<sup>1</sup> and Towe Wang<sup>1,\*</sup>

<sup>1</sup>*Department of Physics, East China Normal University,  
Shanghai 200241, China*

(Dated: March 26, 2019)

In non-canonical two-field inflation models, deviations from the canonical model can be captured by a parameter  $\xi$ . We show this parameter is usually one half of the slow-roll order and analytically calculate the primordial power spectra to the precision of order  $\xi^2$ . The super-horizon perturbations are studied with an improved method, which gives a correction of order  $\xi$ . Three typical examples demonstrate that our analytical formulae of power spectra fit well with numerical simulation.

## I. MOTIVATION

Popularly taken as one ingredient of the Big Bang theory, inflation [1] has become the prevailing paradigm for studying the very early phase of our Universe. However, we are still far from the standard model of inflation. Observationally, inflation will be further tested or revealed in details by accumulating data of the cosmic microwave background, the baryon acoustic oscillation, etc [2]. Theoretically, a consensus has not been attained on the inflationary Lagrangian. Besides the simplest single-field model of inflation [3, 4] and its variants [5, 6], there are a large number of extended models, among which we will study in this paper the generalized two-field inflation model [7–13] described by an action of the form

$$S = \int d^4x \sqrt{-g} \left[ \frac{M_P^2}{2} R - \frac{1}{2} (\partial_\mu \phi)(\partial^\mu \phi) - \frac{e^{2b(\phi)}}{2} (\partial_\mu \chi)(\partial^\mu \chi) - V(\phi, \chi) \right]. \quad (1)$$

Here  $M_P = (8\pi G)^{-1/2}$  is the reduced Plank mass, and  $b(\phi)$  is a function of scalar field  $\phi$ . Thus the other scalar field  $\chi$  acquires a non-standard kinetic term. In the special case  $b = -\phi/(\sqrt{6}M_P)$ , this model is equivalent to the  $f(\chi, R)$  generalized gravity [14–17] and the generalized hybrid metric-Palatini gravity [18].

One conventional assumption made in the literature [10–13] is that  $M_P^2 b_\phi^2 \ll 1$ , which unfortunately does not hold in the interesting case  $b = -\phi/(\sqrt{6}M_P)$ . For instance, in reference [12], the parameter  $\xi = \sqrt{2}b_\phi M_P \sqrt{\epsilon}$  is introduced and treated “on the same footing as the other slow-roll parameters”, where  $\epsilon$  is the Hubble slow-roll parameter defined in (13). Under this assumption, reference [12] kept only the terms linear in  $\xi$ ,  $\epsilon$  or  $\eta$  and developed a series of elegant formulae for inflation model (1).

Taking  $b = -\phi/(\sqrt{6}M_P)$ , one can directly see that  $\xi = -\sqrt{2\epsilon/3}$ . In this case,  $\xi$  is of one half order of the slow-roll parameter  $\epsilon$ , hence  $\xi^2$  should be taken on the same footing with  $\epsilon$  in a consistent analysis. Our motivation in this paper is to take  $\xi^2$  terms into consideration and improve precision of the results of reference [12].

Our final results differ from reference [12] even in the first order of  $\xi$ , because we make another improvement. As will be clarified in appendix C, in the old routine [10, 12, 19, 20], the super-horizon perturbations are studied with two second-order differential equations. Instead, in our treatment, super-horizon perturbations are studied with one first-order differential equation and one second-order differential equation. In both methods, the second-order derivative terms are then discarded in  $\mathcal{O}(\xi)$  analysis.

The plan of the paper is as follows. In section II we write down the background equations as well as the slow-roll conditions. In section III, we evolve the perturbations analytically inside and outside the horizon, taking  $\xi^2$  terms into account. For several specific examples, our analytical formulae are confronted with numerical results in section IV. In section V, we comment on a few subtleties. Some technical details are relegated to appendices A and B, in which respectively the matrix (43) is diagonalized and the Hankel function (58) is expanded in the Taylor’s series. Appendix C is devoted to  $\mathcal{O}(\xi^2)$  corrections for the old routine of super-horizon evolution.

---

\* Electronic address: twang@phy.ecnu.edu.cn

## II. BACKGROUND EQUATIONS AND SLOW-ROLL CONDITIONS

In this section we will investigate the evolution of the background under the slow-roll approximation. Starting with action (1), in subsection II A we will write down the background equations and rearrange them along and orthogonal to the trajectory in field space. In subsection II B, we will scrutinize the slow-roll condition and put forward a problem related to  $f(\phi, R)$  inflation.

### A. Background equations of motion

With the background metric

$$ds^2 = -dt^2 + a(t)^2 d\vec{x}^2, \quad (2)$$

the action (1) leads to the following equations of motion for the scalar fields

$$\ddot{\phi} + 3H\dot{\phi} + V_\phi = b_\phi e^{2b}\dot{\chi}^2, \quad (3)$$

$$\ddot{\chi} + (3H + 2b_\phi\dot{\phi})\dot{\chi} + e^{-2b}V_\chi = 0 \quad (4)$$

and the Friedmann equations

$$H^2 = \frac{1}{3M_p^2} \left[ \frac{1}{2}\dot{\phi}^2 + \frac{e^{2b}}{2}\dot{\chi}^2 + V \right], \quad (5)$$

$$\dot{H} = -\frac{1}{2M_p^2} \left[ \dot{\phi}^2 + e^{2b}\dot{\chi}^2 \right]. \quad (6)$$

The last equation is not independent from the others. Here  $t$  denotes the physical time, and a dot denotes the derivative with respect to it. Later on, we will need the conformal time  $\tau$ , with respect to which the derivatives are denoted by primes.

To study the evolution of perturbations, it is more convenient to introduce the average and orthogonal fields, corresponding to tangent and orthogonal directions of the trajectory in field space. Perturbations of the average and orthogonal fields  $\delta\sigma$ ,  $\delta s$  are related to perturbations of the primitive fields  $\delta\phi$ ,  $\delta\chi$  by

$$\delta\sigma \equiv \cos\theta\delta\phi + \sin\theta e^b\delta\chi, \quad \delta s \equiv -\sin\theta\delta\phi + \cos\theta e^b\delta\chi, \quad (7)$$

where

$$\cos\theta \equiv \frac{\dot{\phi}}{\dot{\sigma}}, \quad \sin\theta \equiv \frac{\dot{\chi}e^b}{\dot{\sigma}}, \quad \dot{\sigma} \equiv \sqrt{\dot{\phi}^2 + e^{2b}\dot{\chi}^2}. \quad (8)$$

In terms of average field  $\sigma$  and angle  $\theta$ , equations (3) and (4) can be put in the form [12]

$$\ddot{\sigma} + 3H\dot{\sigma} + V_\sigma = 0, \quad (9)$$

$$\dot{\theta} = -\frac{V_s}{\dot{\sigma}} - b_\phi\dot{\sigma}\sin\theta. \quad (10)$$

By definition (7), the first-order derivatives of the potential are related by

$$\begin{aligned} V_\sigma &= V_\phi \cos\theta + e^{-b}V_\chi \sin\theta, \\ V_s &= -V_\phi \sin\theta + e^{-b}V_\chi \cos\theta, \end{aligned} \quad (11)$$

and the second-order derivatives of the potential are related by

$$\begin{aligned} V_{\sigma\sigma} &= V_{\phi\phi}c_\theta^2 + e^{-2b}V_{\chi\chi}s_\theta^2 + e^{-b}V_{\phi\chi}s_\theta c_\theta + e^{-b}V_{\chi\phi}s_\theta c_\theta, \\ V_{\sigma s} &= -V_{\phi\phi}s_\theta c_\theta + e^{-2b}V_{\chi\chi}s_\theta c_\theta + e^{-b}V_{\phi\chi}c_\theta^2 - e^{-b}V_{\chi\phi}s_\theta^2, \\ V_{ss} &= V_{\phi\phi}s_\theta^2 + e^{-2b}V_{\chi\chi}c_\theta^2 - e^{-b}V_{\phi\chi}s_\theta c_\theta - e^{-b}V_{\chi\phi}s_\theta c_\theta. \end{aligned} \quad (12)$$

Hereafter we will use notations  $s_\theta \equiv \sin\theta$ ,  $c_\theta \equiv \cos\theta$  for brevity.

## B. Slow-roll conditions and $\xi$ -problem

Similar to the single-field inflation, it is customary to define the slow-roll parameters as [10]

$$\begin{aligned}\epsilon &= -\frac{\dot{H}}{H^2}, \\ \eta_{\phi\phi} &= \frac{M_p^2 V_{\phi\phi}}{V}, \quad \eta_{\phi\chi} = \frac{M_p^2 e^{-b} V_{\phi\chi}}{V}, \quad \eta_{\chi\chi} = \frac{M_p^2 e^{-2b} V_{\chi\chi}}{V}, \\ \eta_{\sigma\sigma} &= \frac{M_p^2 V_{\sigma\sigma}}{V}, \quad \eta_{\sigma s} = \frac{M_p^2 V_{\sigma s}}{V}, \quad \eta_{ss} = \frac{M_p^2 V_{ss}}{V}.\end{aligned}\tag{13}$$

Then the slow-roll conditions are given by

$$\epsilon \ll 1,\tag{14}$$

$$|\eta_{\phi\phi}| \ll 1, \quad |\eta_{\phi\chi}| \ll 1, \quad |\eta_{\chi\chi}| \ll 1,\tag{15}$$

$$|\eta_{\sigma\sigma}| \ll 1, \quad |\eta_{\sigma s}| \ll 1, \quad |\eta_{ss}| \ll 1.\tag{16}$$

In terms of slow-roll parameters, relation (12) can be reexpressed as

$$\begin{aligned}\eta_{\sigma\sigma} &= \eta_{\phi\phi} c_\theta^2 + \eta_{\chi\chi} s_\theta^2 + 2\eta_{\phi\chi} s_\theta c_\theta, \\ \eta_{\sigma s} &= -\eta_{\phi\phi} s_\theta c_\theta + \eta_{\chi\chi} s_\theta c_\theta + \eta_{\phi\chi} (c_\theta^2 - s_\theta^2), \\ \eta_{ss} &= \eta_{\phi\phi} s_\theta^2 + \eta_{\chi\chi} c_\theta^2 - 2\eta_{\phi\chi} s_\theta c_\theta.\end{aligned}\tag{17}$$

Hence the slow-roll conditions (15) and (16) are equivalent to each other.

As we will see in the next section,  $V_s/\dot{\sigma}$  appears frequently in the coefficients of perturbation equations. In the slow-roll approximation, one can utilize the background equations to prove the following relation [8, 12]

$$\frac{V_s}{H\dot{\sigma}} = \eta_{\sigma s} - \frac{\dot{\sigma} b_\phi s_\theta^3}{H} = \eta_{\sigma s} - \sqrt{2\epsilon} M_P b_\phi s_\theta^3.\tag{18}$$

On the right-hand side, the first term is of the slow-roll order, while the second term is proportional to  $\sqrt{\epsilon}$ , i.e. a half order of slow roll. To tame this problem, reference [12] introduced a parameter  $\xi = \sqrt{2} b_\phi M_P \sqrt{\epsilon}$  and treated it ‘‘on the same footing as the other slow-roll parameters’’. Under this assumption, reference [12] kept only terms linear in  $\xi$ ,  $\epsilon$  or  $\eta$  and developed a series of elegant formulae for inflation model (1).

In theories such the  $f(\chi, R)$  generalized gravity [14–17] and the generalized hybrid metric-Palatini gravity [18], one has to deal with models of the form  $b = -\phi/(\sqrt{6}M_P)$ . In that case  $\xi = -\sqrt{2\epsilon/3}$ , and  $\xi^2$  is of order  $\epsilon$ . Therefore, it would be interesting to take  $\xi^2$  terms into consideration and refine the analysis of reference [12]. This will be done in the following sections.

Throughout this paper, we will assume that the slow-roll parameters vary sufficiently slowly during inflation. This is confirmed by our numerical examples in section IV.

## III. ANALYTICAL STUDY OF PERTURBATIONS INCLUDING $\xi^2$ TERMS

### A. Perturbation equations

In the longitudinal gauge, the metric with the scalar-type perturbation is of the form

$$ds^2 = -(1 + 2\Phi)dt^2 + a^2(1 - 2\Phi)d\vec{x}^2,\tag{19}$$

while the curvature and entropy perturbations are defined by

$$\mathcal{R} \equiv \frac{H}{\dot{\sigma}} Q_\sigma, \quad \mathcal{S} \equiv \frac{H}{\dot{\sigma}} \delta s\tag{20}$$

in which

$$Q_\sigma \equiv \delta\sigma + \frac{\dot{\sigma}}{H}\Phi.\tag{21}$$

In reference [12], it has been shown that perturbations  $Q_\sigma$  and  $\delta s$  are subject to the constraint

$$\dot{\sigma}\dot{Q}_\sigma + \left(3H + \frac{\dot{H}}{H}\right)\dot{\sigma}Q_\sigma + V_\sigma Q_\sigma + 2V_s\delta s = -\frac{2M_P^2 k^2}{a^2}\Phi \quad (22)$$

and the equations of motion

$$\ddot{Q}_\sigma + 3H\dot{Q}_\sigma + \left(\frac{k^2}{a^2} + C_{\sigma\sigma}\right)Q_\sigma + \frac{2V_s}{\dot{\sigma}}\delta\dot{s} + C_{\sigma s}\delta s = 0, \quad (23)$$

$$\ddot{\delta s} + 3H\dot{\delta s} + \left(\frac{k^2}{a^2} + C_{ss}\right)\delta s - \frac{2V_s}{\dot{\sigma}}\dot{Q}_\sigma + C_{s\sigma}Q_\sigma = 0, \quad (24)$$

where the coefficients are

$$\begin{aligned} C_{\sigma\sigma} &= V_{\sigma\sigma} - \left(\frac{V_s}{\dot{\sigma}}\right)^2 + \frac{2\dot{\sigma}V_\sigma}{M_P^2 H} + \frac{3\dot{\sigma}^2}{M_P^2} - \frac{\dot{\sigma}^4}{2M_P^4 H^2} - b_\phi [s_\theta^2 c_\theta V_\sigma + (c_\theta^2 + 1)s_\theta V_s], \\ C_{\sigma s} &= 6H\frac{V_s}{\dot{\sigma}} + \frac{2V_\sigma V_s}{\dot{\sigma}^2} + 2V_{\sigma s} + \frac{\dot{\sigma}V_s}{M_P^2 H} + 2b_\phi (s_\theta^3 V_\sigma - c_\theta^3 V_s), \\ C_{ss} &= V_{ss} - \left(\frac{V_s}{\dot{\sigma}}\right)^2 + b_\phi(1 + s_\theta^2)c_\theta V_\sigma + b_\phi c_\theta^2 s_\theta V_s - \dot{\sigma}^2 (b_{\phi\phi} + b_\phi^2), \\ C_{s\sigma} &= -6H\frac{V_s}{\dot{\sigma}} - \frac{2V_\sigma V_s}{\dot{\sigma}^2} + \frac{\dot{\sigma}V_s}{M_P^2 H}. \end{aligned} \quad (25)$$

In terms of slow-roll parameters  $\epsilon$ ,  $\eta$  and  $\xi$ , these coefficients can be rewritten under the slow-roll approximation as

$$\begin{aligned} C_{\sigma\sigma} &= H^2 (3\xi c_\theta s_\theta^2 - 6\epsilon + 3\eta_{\sigma\sigma} + 2\xi^2 c_\theta^2 s_\theta^4) + \mathcal{O}(\epsilon^2, \eta^2, \xi^3, \epsilon\eta, \epsilon\xi, \eta\xi) \\ C_{\sigma s} &= H^2 (-6\xi s_\theta^3 + 6\eta_{\sigma s} + 2\xi^2 c_\theta^3 s_\theta^3) + \mathcal{O}(\epsilon^2, \eta^2, \xi^3, \epsilon\eta, \epsilon\xi, \eta\xi) \\ C_{ss} &= H^2 [-3\xi c_\theta(1 + s_\theta^2) + 3\eta_{ss} - \xi^2 - \xi^2 s_\theta^4] + \mathcal{O}(\epsilon^2, \eta^2, \xi^3, \epsilon\eta, \epsilon\xi, \eta\xi) \\ C_{s\sigma} &= \mathcal{O}(\epsilon^2, \eta^2, \xi^3, \epsilon\eta, \epsilon\xi, \eta\xi). \end{aligned} \quad (26)$$

With the perturbation equations of motion (23) and (24) at hand, we will study the evolution of perturbations  $Q_\sigma$ ,  $\delta s$  along the timeline, where the physical wavelength  $a/k$  grows together with the scale factor  $a$ . At the very beginning, the physical wavenumber is much bigger than the Hubble parameter  $k/a \gg H$ . Therein  $aQ_\sigma$ ,  $a\delta s$  behave as free-field fluctuations, living in a Minkowski vacuum. We will discuss the Minkowski-like vacuum as initial conditions in subsection III B. Starting from such initial conditions, the evolution of perturbations during inflation can be roughly divided into two stages: the sub-horizon stage  $k/(aH) \gtrsim 1$  and the super-horizon stage  $k/(aH) \lesssim 1$ . Perturbation evolution during the two stages will be investigated in subsections III C and III D. It is customary to mark the timeline with the number of e-folds. In our convention of notations, the number of e-folds after Hubble crossing is defined by

$$N = \ln \frac{a}{a_*}. \quad (27)$$

Hereafter the quantities with a subscript star are evaluated at Hubble crossing  $k = a_*H$ .

## B. Initial conditions

Before studying the evolution of perturbations, we should set their initial conditions. At the very beginning of inflation, the physical wavelength  $a/k$  is far smaller than the radius of Hubble horizon  $1/H$ , i.e.  $k/a \gg H$ , so the coupling terms and mass terms become negligible in equations (23) and (24), which reduce to the equations of motion of free harmonic oscillators. Then as initial conditions, the fluctuations  $aQ_\sigma$  and  $a\delta s$  can be quantized as free fields. That is to say, at the initial time  $\tau_i \rightarrow -\infty$ , we have [21]

$$Q_\sigma(\tau_i) \simeq \frac{e^{-ik\tau_i}}{a(\tau_i)\sqrt{2k}}e_\sigma(k), \quad \delta s(\tau_i) \simeq \frac{e^{-ik\tau_i}}{a(\tau_i)\sqrt{2k}}e_s(k). \quad (28)$$

Here the independent Gaussian random variables  $e_\sigma$  and  $e_s$  are orthogonally normalized

$$\langle e_I(k) \rangle = 0, \quad \langle e_I(k)e_J^*(k') \rangle = \delta_{IJ}\delta^{(3)}(k - k') \quad (29)$$

with  $I, J = \sigma, s$ .

In the next subsection, at Hubble crossing, we will need two other Gaussian random variables  $e_1$  and  $e_2$ , which are related to  $e_\sigma$  and  $e_s$  via

$$\begin{pmatrix} e_1 \\ e_2 \end{pmatrix} = \begin{pmatrix} \cos \Theta_* & \sin \Theta_* \\ \sin \Psi_* & \cos \Psi_* \end{pmatrix} \begin{pmatrix} e_\sigma \\ e_s \end{pmatrix}, \quad (30)$$

Note that  $e_1, e_2, e_\sigma, e_s$  are time-independent variables, and  $\Theta_*, \Psi_*$  are also time-independent. This transformation matrix generalizes the rotation matrix in references [12, 22]. Especially, when  $\Psi_* = -\Theta_*$ , it reduces to the relation in [12]. In our general form,  $e_1$  and  $e_2$  are not always orthogonal to each other. Instead,

$$\langle e_A(k) e_B^*(k') \rangle = \Delta_{AB} \delta^{(3)}(k - k') \quad (31)$$

with  $A, B = 1, 2$  and

$$\Delta_{AB} \equiv \begin{cases} 1, & A = B; \\ \sin(\Theta_* + \Psi_*), & A \neq B. \end{cases} \quad (32)$$

### C. Sub-horizon evolution and horizon crossing

In this subsection, we will study the dynamical evolution of perturbations  $Q_\sigma$  and  $\delta s$  from deep inside the Hubble horizon to Hubble crossing. Introducing variables

$$u_\sigma = aQ_\sigma, \quad u_s = a\delta s, \quad (33)$$

and using the conformal time  $\tau$ , we can rewrite equations (23) and (24) as

$$\begin{aligned} u''_\sigma + \frac{2V_s}{\dot{\sigma}} a u'_\sigma + \left[ k^2 - \frac{a''}{a} + a^2 C_{\sigma\sigma} \right] u_\sigma + \left[ -\frac{2V_s}{\dot{\sigma}} a' + a^2 C_{\sigma s} \right] u_s &= 0, \\ u''_s - \frac{2V_s}{\dot{\sigma}} a u'_\sigma + \left[ k^2 - \frac{a''}{a} + a^2 C_{ss} \right] u_s + \left[ \frac{2V_s}{\dot{\sigma}} a' + a^2 C_{s\sigma} \right] u_\sigma &= 0. \end{aligned} \quad (34)$$

The four coefficients  $C_{IJ}$  have been given by equations (25). Unlike reference [12], in the following discussion, we will keep terms of  $\mathcal{O}(\epsilon, \eta, \xi)$  and  $\mathcal{O}(\xi^2)$ .

From definition  $d\tau = dt/a$ , we can get some useful relations

$$\begin{aligned} \tau &= -\frac{1+\epsilon}{Ha}, \quad a' = a^2 H, \\ \frac{1}{a^2} &\simeq H^2 \tau^2 (1-2\epsilon), \quad \frac{a''}{a} \simeq \frac{2+3\epsilon}{\tau^2}, \end{aligned} \quad (35)$$

which will be utilized without mention hereafter. Then the perturbation equations can be put in the matrix form

$$\left[ \left( \frac{d^2}{d\tau^2} + k^2 - \frac{2+3\epsilon}{\tau^2} \right) \mathbf{I} + 2\mathbf{E} \frac{1}{\tau} \frac{d}{d\tau} + \mathbf{M} \frac{1}{\tau^2} \right] \begin{pmatrix} u_\sigma \\ u_s \end{pmatrix} = 0, \quad (36)$$

where  $\mathbf{I}$  is the unitary matrix, and matrices  $\mathbf{E}, \mathbf{M}$  are

$$\begin{aligned} \mathbf{E} &= \begin{pmatrix} 0 & -(1+\epsilon)(\eta_{\sigma s} - \xi s_\theta^3) \\ (1+\epsilon)(\eta_{\sigma s} - \xi s_\theta^3) & 0 \end{pmatrix}, \\ \mathbf{M} &= \begin{pmatrix} H^{-2} C_{\sigma\sigma} (1+\epsilon)^2 & (-2\eta_{\sigma s} + 2\xi s_\theta^3 + H^{-2} C_{\sigma s}) (1+\epsilon)^2 \\ (2\eta_{\sigma s} - 2\xi s_\theta^3 + H^{-2} C_{s\sigma}) (1+\epsilon)^2 & H^{-2} C_{ss} (1+\epsilon)^2 \end{pmatrix}. \end{aligned} \quad (37)$$

The above system of perturbation equations can be succinctly written as

$$u'' + 2\mathbf{L}u' + \mathbf{Q}u = 0 \quad (38)$$

if we take notations

$$u = \begin{pmatrix} u_\sigma \\ u_s \end{pmatrix}, \quad \mathbf{L} = \frac{1}{\tau} \mathbf{E}, \quad \mathbf{Q} = \left( k^2 - \frac{2+3\epsilon}{\tau^2} \right) \mathbf{I} + \frac{1}{\tau^2} \mathbf{M}. \quad (39)$$

It is remarkable that matrices  $\mathbf{E}$ ,  $\mathbf{L}$  here are exactly the same as them in reference [12]. As argued in reference [12], there is always an orthogonal matrix  $\mathbf{R}$  obeying the differential equation

$$\frac{d}{d\tau}\mathbf{R} = -\mathbf{L}\mathbf{R}, \quad (40)$$

and  $\mathbf{R}$  is slowly varying because  $\mathbf{E}$  is linear in slow-roll parameters. Consequently, in terms of  $v = \mathbf{R}^{-1}u$ , the system of perturbation equations can be further rewritten as

$$v'' + \mathbf{R}^{-1}(-\mathbf{L}^2 - \mathbf{L}' + \mathbf{Q})\mathbf{R}v = 0, \quad (41)$$

where  $\mathbf{L}' = d\mathbf{L}/d\tau$ . From relation  $\mathbf{L} = \mathbf{E}/\tau$ , it is easy to see

$$-\mathbf{L}^2 - \mathbf{L}' = -\frac{\mathbf{E}^2}{\tau^2} + \frac{\mathbf{E}}{\tau^2} \quad (42)$$

if slow-roll parameters vary sufficiently slowly. Here we have kept the  $\mathbf{E}^2$  term in order to retrieve  $\mathcal{O}(\xi^2)$  terms.

To proceed, we have to decouple the system (41) into two independent equations. That is equivalent to diagonalizing the coefficient matrix of  $v$  through a similarity transformation. For this purpose, we should diagonalize the following matrix

$$\begin{aligned} \tilde{\mathbf{M}} &= -\mathbf{E}^2 + \mathbf{E} + \mathbf{M} \\ &= \begin{pmatrix} 3\xi c_\theta s_\theta^2 - 6\epsilon + 3\eta_{\sigma\sigma} & -3\xi s_\theta^3 + 3\eta_{\sigma s} \\ -3\xi s_\theta^3 + 3\eta_{\sigma s} & -3\xi c_\theta - 3\xi c_\theta s_\theta^2 + 3\eta_{ss} \end{pmatrix} + \begin{pmatrix} \xi^2 s_\theta^4 + \xi^2 c_\theta^2 s_\theta^4 & 2\xi^2 c_\theta^3 s_\theta^3 \\ 0 & -\xi^2 - \xi^2 c_\theta^2 s_\theta^4 \end{pmatrix}, \end{aligned} \quad (43)$$

where we have kept terms of  $\mathcal{O}(\epsilon, \eta, \xi)$  and  $\mathcal{O}(\xi^2)$ . The second term, which is proportional to  $\xi^2$ , has been neglected in reference [12]. In this paper, as we have explained in subsection II B,  $\xi^2$  is supposed to be of order  $\epsilon$  and thus nonnegligible. This makes our investigation more challenging than [12]. In particular, due to the second term, the above matrix is no longer symmetric and hence cannot be diagonalized through an orthogonal similarity transformation. Fortunately, since  $\tilde{\mathbf{M}}$  has analytically two distinct eigenvalues  $\tilde{\lambda}_1, \tilde{\lambda}_2$  as given in appendix A, we can still diagonalize the matrix through a similarity transformation. Remember that if there are exactly  $n$  distinct eigenvalues in an  $n \times n$  matrix, then this matrix is diagonalizable. However, such a similarity transformation is not always an orthogonal transformation. That is why in subsection III B the variables  $e_1, e_2$  are not necessarily orthogonal to each other. The details are given below.

Since the slow-roll parameters are approximately constant, one can diagonalize matrix  $\tilde{\mathbf{M}}$  with a time-independent matrix  $\tilde{\mathbf{R}}_*$  as

$$\tilde{\mathbf{R}}_*^{-1}\tilde{\mathbf{M}}\tilde{\mathbf{R}}_* = \text{Diag}(\tilde{\lambda}_1, \tilde{\lambda}_2). \quad (44)$$

The values of  $\tilde{\lambda}_1, \tilde{\lambda}_2$  are given by equations (A3). Without loss of generality and for later convenience, we parameterize the inverse of  $\tilde{\mathbf{R}}_*$  with two angles  $\Theta_*, \Psi_*$  in the following form

$$\tilde{\mathbf{R}}_*^{-1} = \begin{pmatrix} \cos \Theta_* & \sin \Theta_* \\ \sin \Psi_* & \cos \Psi_* \end{pmatrix}. \quad (45)$$

From  $\tilde{\mathbf{R}}_*\tilde{\mathbf{R}}_*^{-1} = \mathbf{I}$ , we can directly write down

$$\tilde{\mathbf{R}}_* = \frac{1}{\cos(\Theta_* + \Psi_*)} \begin{pmatrix} \cos \Psi_* & -\sin \Theta_* \\ -\sin \Psi_* & \cos \Theta_* \end{pmatrix}. \quad (46)$$

If we further transform  $v$  into

$$w = \tilde{\mathbf{R}}_*^{-1}\mathbf{R}_*v, \quad (47)$$

then because  $\mathbf{R}$  varies slowly, we have approximately  $w \simeq \tilde{\mathbf{R}}_*^{-1}u$ , and perturbation equations (41) can be decoupled into two independent equations of the form

$$w''_A + [k^2 - \frac{1}{\tau^2}(2 + 3\lambda_A)]w_A = 0 \quad (48)$$

with  $A = 1, 2$  and

$$\lambda_A = \epsilon - \frac{\tilde{\lambda}_A}{3}. \quad (49)$$

For matrix (43), in appendix A we present the eigenvalues  $\tilde{\lambda}_1$  and  $\tilde{\lambda}_2$  as well as some trigonometric functions of  $\Psi_*$  and  $\Theta_*$ .

Keep in mind that  $\tilde{\mathbf{R}}_*$  is not necessarily an orthogonal matrix. As a result, the solutions  $w_1, w_2$  of (48) are not orthogonal to each other. This introduces extra complications to our study. To see this, let us utilize the notation

$$\mu_A = \sqrt{\frac{9}{4} + 3\lambda_A} \quad (50)$$

to write down the solutions of (48) as [22]

$$w_A = \frac{\sqrt{\pi}}{2} e^{i(\mu_A+1/2)\pi/2} \sqrt{-\tau} H_{\mu_A}^{(1)}(-k\tau) e_A(k) \quad (51)$$

where  $H_{\mu}^{(1)}$  is the Hankel function of the first kind of order  $\mu$ , and the variables  $e_1, e_2$  have been defined in subsection III B. Clearly  $\langle w_1^\dagger w_2 \rangle \neq 0$  because of equation (31). This will have significant implications for the calculation of power spectra.

Considering that  $w \simeq \tilde{\mathbf{R}}_*^{-1} u$  at Hubble crossing, we can prove

$$\begin{aligned} aQ_\sigma &= \frac{\cos \Psi_*}{\cos(\Theta_* + \Psi_*)} w_1 - \frac{\sin \Theta_*}{\cos(\Theta_* + \Psi_*)} w_2, \\ a\delta s &= -\frac{\sin \Psi_*}{\cos(\Theta_* + \Psi_*)} w_1 + \frac{\cos \Theta_*}{\cos(\Theta_* + \Psi_*)} w_2 \end{aligned}$$

and immediately write down their correlations

$$\begin{aligned} a^2 \langle Q_\sigma^\dagger Q_\sigma \rangle &= \frac{\cos^2 \Psi_*}{\cos^2(\Theta_* + \Psi_*)} \langle w_1^\dagger w_1 \rangle + \frac{\sin^2 \Theta_*}{\cos^2(\Theta_* + \Psi_*)} \langle w_2^\dagger w_2 \rangle - \frac{\cos \Psi_* \sin \Theta_*}{\cos^2(\Theta_* + \Psi_*)} \left( \langle w_1^\dagger w_2 \rangle + \langle w_2^\dagger w_1 \rangle \right), \\ a^2 \langle \delta s^\dagger \delta s \rangle &= \frac{\sin^2 \Psi_*}{\cos^2(\Theta_* + \Psi_*)} \langle w_1^\dagger w_1 \rangle + \frac{\cos^2 \Theta_*}{\cos^2(\Theta_* + \Psi_*)} \langle w_2^\dagger w_2 \rangle - \frac{\sin \Psi_* \cos \Theta_*}{\cos^2(\Theta_* + \Psi_*)} \left( \langle w_1^\dagger w_2 \rangle + \langle w_2^\dagger w_1 \rangle \right), \\ a^2 \langle Q_\sigma^\dagger \delta s \rangle &= -\frac{\cos \Psi_* \sin \Psi_*}{\cos^2(\Theta_* + \Psi_*)} \langle w_1^\dagger w_1 \rangle - \frac{\cos \Theta_* \sin \Theta_*}{\cos^2(\Theta_* + \Psi_*)} \langle w_2^\dagger w_2 \rangle + \frac{\sin \Theta_* \sin \Psi_*}{\cos^2(\Theta_* + \Psi_*)} \langle w_2^\dagger w_1 \rangle + \frac{\cos \Psi_* \cos \Theta_*}{\cos^2(\Theta_* + \Psi_*)} \langle w_1^\dagger w_2 \rangle. \end{aligned} \quad (52)$$

Remember that  $Q_\sigma$  and  $\delta s$  are related to curvature perturbation  $\mathcal{R}$  and entropy perturbation  $\mathcal{S}$  respectively by (20). With the above correlations, in principle one can compute the power spectra of  $\mathcal{R}$  and  $\mathcal{S}$  as well as their correlation spectrum by definitions

$$\begin{aligned} \langle \mathcal{R}_k^* \mathcal{R}_{k'} \rangle &= \frac{2\pi^2}{k^3} \mathcal{P}_{\mathcal{R}}(k) \delta^{(3)}(k - k'), \\ \langle \mathcal{S}_k^* \mathcal{S}_{k'} \rangle &= \frac{2\pi^2}{k^3} \mathcal{P}_{\mathcal{S}}(k) \delta^{(3)}(k - k'), \\ \langle \mathcal{R}_k^* \mathcal{S}_{k'} \rangle &= \frac{2\pi^2}{k^3} \mathcal{C}_{\mathcal{R}\mathcal{S}}(k) \delta^{(3)}(k - k') \end{aligned} \quad (53)$$

and further more the relative correlation coefficient

$$\tilde{\mathcal{C}} = \frac{\mathcal{C}_{\mathcal{R}\mathcal{S}}}{\sqrt{\mathcal{P}_{\mathcal{R}}\mathcal{P}_{\mathcal{S}}}}. \quad (54)$$

But in practice the computation is rather complicated when  $\Psi_* \neq -\Theta_*$  and  $\langle w_1^\dagger w_2 \rangle \neq 0$ , because we want to keep  $\mathcal{O}(\xi^2)$  corrections. To accomplish the task, we will expand the spectra to  $\mathcal{O}(\epsilon, \eta, \xi)$  and  $\mathcal{O}(\xi^2)$  at several e-folds after Hubble crossing, that is  $k/(aH) \ll 1$  or equivalently  $-k\tau \ll 1$ .

From equations (A3), we can see the leading-order term in  $\lambda_A$  is linear in  $\xi$ , so in our series expansion below we will keep  $\mathcal{O}(\lambda_A^2)$  terms. For instance,

$$\mu_A \simeq \frac{3}{2} + \lambda_A - \frac{1}{3} \lambda_A^2. \quad (55)$$

In terms of the gamma function  $\Gamma(\mu)$  and Bessel functions of the first kind  $J_\mu(x)$ , the Hankel function  $H_\mu^{(1)}(x)$  can be expressed as

$$\begin{aligned} H_\mu^{(1)}(x) &= \frac{J_{-\mu}(x) - e^{-i\mu\pi} J_\mu(x)}{i \sin(\mu\pi)}, \\ J_\mu(x) &= \sum_{m=0}^{\infty} \frac{(-1)^m}{m! \Gamma(m + \mu + 1)} \left(\frac{x}{2}\right)^{2m + \mu}. \end{aligned} \quad (56)$$

Apparently, when  $\mu > 0$  and  $x \ll 1$ , the Hankel function  $H_\mu^{(1)}(x)$  is divergent as  $x^{-\mu}$ . If we renormalize  $H_{\mu_A}^{(1)}(x)$  as

$$\tilde{H}_{\mu_A}^{(1)}(x) \equiv x^{\mu_A} H_{\mu_A}^{(1)}(x) \quad (57)$$

and take (55) into account, then  $\tilde{H}_{\mu_A}^{(1)}(x)$  can be expanded to  $\mathcal{O}(\lambda_A^2)$  as

$$\tilde{H}_{\mu_A}^{(1)}(x) \simeq \tilde{H}_{3/2}^{(1)}(x) + \left( \lambda_A - \frac{\lambda_A^2}{3} \right) \frac{d\tilde{H}_\mu^{(1)}(x)}{d\mu} \Big|_{\mu=3/2} + \frac{\lambda_A^2}{2} \frac{d^2\tilde{H}_\mu^{(1)}(x)}{d\mu^2} \Big|_{\mu=3/2}. \quad (58)$$

This leads to

$$\begin{aligned} & \frac{\pi}{2} x^3 H_{\mu_A}^{(1)*}(x) H_{\mu_B}(x) \\ & \simeq \frac{\pi}{2} x^3 \left| H_{3/2}^{(1)}(x) \right|^2 \left[ 1 + \left( \lambda_A - \frac{\lambda_A^2}{3} \right) f(x) + \frac{\lambda_A^2}{2} g(x) \right] \left[ 1 + \left( \lambda_B - \frac{\lambda_B^2}{3} \right) f(x) + \frac{\lambda_B^2}{2} g(x) \right] \\ & \simeq (1+x^2) \left[ 1 + \left( \lambda_A + \lambda_B - \frac{\lambda_A^2}{3} - \frac{\lambda_B^2}{3} \right) f(x) + \lambda_A \lambda_B f^2(x) + \frac{1}{2} (\lambda_A^2 + \lambda_B^2) g(x) \right]. \end{aligned} \quad (59)$$

In the expression we have introduced

$$\begin{aligned} f(x) &= \frac{1}{\tilde{H}_{3/2}^{(1)}(x)} \frac{d\tilde{H}_\mu^{(1)}(x)}{d\mu} \Big|_{\mu=3/2} \\ &\simeq 2 - \ln 2 - \gamma - \frac{2x^2}{2+x^2} \\ &\simeq 0.7296 - x^2, \\ g(x) &= \frac{1}{\tilde{H}_{3/2}^{(1)}(x)} \frac{d^2\tilde{H}_\mu^{(1)}(x)}{d\mu^2} \Big|_{\mu=3/2} \\ &\simeq \frac{\pi^2}{2} + (\ln 2 + \gamma) \left( -4 + \ln 2 + \gamma + \frac{4x^2}{2+x^2} \right) \\ &\simeq 1.4672 + 2.5407x^2, \end{aligned} \quad (60)$$

where  $\gamma \simeq 0.5772$  is the Euler-Mascheroni constant. The details for evaluating  $f(x)$  and  $g(x)$  are relegated to appendix B.

With this result at hand, using the modified normalization condition (31), we can work out the correlations of the two solutions (51) to  $\mathcal{O}(\lambda_A^2)$ , yielding

$$\begin{aligned} \langle w_A^\dagger(k) w_B(k') \rangle &= \frac{\pi}{4} (-\tau) e^{i\pi(\mu_B - \mu_A)/2} H_{\mu_A}^*(-k\tau) H_{\mu_B}(-k\tau) \Delta_{AB} \delta^{(3)}(k - k') \\ &\simeq e^{i\pi(\mu_B - \mu_A)/2} \frac{1}{2k} \frac{1}{k^2 \tau^2} (1 + k^2 \tau^2) \left[ 1 + \left( \lambda_A + \lambda_B - \frac{\lambda_A^2}{3} - \frac{\lambda_B^2}{3} \right) f(-k\tau) + \lambda_A \lambda_B f^2(-k\tau) \right. \\ &\quad \left. + \frac{1}{2} (\lambda_A^2 + \lambda_B^2) g(-k\tau) \right] \Delta_{AB} \delta^{(3)}(k - k') \end{aligned} \quad (61)$$

with  $\Delta_{AB}$  defined by (32). Note here

$$\begin{aligned} e^{i\pi(\mu_B - \mu_A)/2} &\simeq 1 + \frac{i\pi}{2} (\mu_B - \mu_A) - \frac{\pi^2}{8} (\mu_B - \mu_A)^2 \\ &\simeq 1 + \frac{i\pi}{2} \left( \lambda_B - \lambda_A - \frac{\lambda_B^2}{3} + \frac{\lambda_A^2}{3} \right) - \frac{\pi^2}{8} (\lambda_B - \lambda_A)^2. \end{aligned} \quad (62)$$

Inserting (61) into equations (52), by definitions (53) we finally obtain the spectra after Hubble crossing

$$\begin{aligned}
\bar{\mathcal{P}}_{\mathcal{R}} &= \left( \frac{H_*^2}{2\pi\dot{\sigma}_*} \right)^2 (1+k^2\tau^2)(1-2\epsilon_*) \left\{ \frac{\cos^2\Psi_* + \sin^2\Theta_*}{\cos^2(\Theta_* + \Psi_*)} + \frac{(6\lambda_1 - 2\lambda_1^2)\cos^2\Psi_* + (6\lambda_2 - 2\lambda_2^2)\sin^2\Theta_*}{3\cos^2(\Theta_* + \Psi_*)} f(-k\tau) \right. \\
&\quad + \frac{\lambda_1^2\cos^2\Psi_* + \lambda_2^2\sin^2\Theta_*}{\cos^2(\Theta_* + \Psi_*)} [f^2(-k\tau) + g(-k\tau)] - \frac{\cos\Psi_*\sin\Theta_*}{\cos^2(\Theta_* + \Psi_*)} \sin(\Theta_* + \Psi_*) \left[ e^{i\pi(\mu_1-\mu_2)/2} + e^{-i\pi(\mu_1-\mu_2)/2} \right] \\
&\quad \times \left[ 1 + \left( \lambda_1 + \lambda_2 - \frac{\lambda_1^2}{3} - \frac{\lambda_2^2}{3} \right) f(-k\tau) + \lambda_1\lambda_2 f^2(-k\tau) + \frac{1}{2}(\lambda_1^2 + \lambda_2^2) g(-k\tau) \right] \left. \right\} \\
&= \left( \frac{H_*^2}{2\pi\dot{\sigma}_*} \right)^2 (1+k^2\tau^2) \left\{ 1 - 2\epsilon_* + \left[ 6\epsilon_* - 2\eta_{\sigma\sigma*} - 2\xi_* s_{\theta*}^2 c_{\theta*} - \frac{2}{3}\xi_*^2(2 + c_{\theta*}^2) s_{\theta*}^4 \right] f(-k\tau) \right. \\
&\quad \left. - \xi_*^2 s_{\theta*}^4 [f^2(-k\tau) + g(-k\tau)] \right\}, \tag{63}
\end{aligned}$$

$$\begin{aligned}
\bar{\mathcal{P}}_{\mathcal{S}} &= \left( \frac{H_*^2}{2\pi\dot{\sigma}_*} \right)^2 (1+k^2\tau^2)(1-2\epsilon_*) \left\{ \frac{\sin^2\Psi_* + \cos^2\Theta_*}{\cos^2(\Theta_* + \Psi_*)} + \frac{(6\lambda_1 - 2\lambda_1^2)\sin^2\Psi_* + (6\lambda_2 - 2\lambda_2^2)\cos^2\Theta_*}{3\cos^2(\Theta_* + \Psi_*)} f(-k\tau) \right. \\
&\quad + \frac{\lambda_1^2\sin^2\Psi_* + \lambda_2^2\cos^2\Theta_*}{\cos^2(\Theta_* + \Psi_*)} [f^2(-k\tau) + g(-k\tau)] - \frac{\sin\Psi_*\cos\Theta_*}{\cos^2(\Theta_* + \Psi_*)} \sin(\Theta_* + \Psi_*) \left[ e^{i\pi(\mu_1-\mu_2)/2} + e^{-i\pi(\mu_1-\mu_2)/2} \right] \\
&\quad \times \left[ 1 + \left( \lambda_1 + \lambda_2 - \frac{\lambda_1^2}{3} - \frac{\lambda_2^2}{3} \right) f(-k\tau) + \lambda_1\lambda_2 f^2(-k\tau) + \frac{1}{2}(\lambda_1^2 + \lambda_2^2) g(-k\tau) \right] \left. \right\} \\
&= \left( \frac{H_*^2}{2\pi\dot{\sigma}_*} \right)^2 (1+k^2\tau^2) \left\{ 1 - 2\epsilon_* + \left[ 2\epsilon_* - 2\eta_{ss*} + 2\xi_*(1 + s_{\theta*}^2) c_{\theta*} - \frac{2}{3}\xi_*^2 s_{\theta*}^2 c_{\theta*}^4 \right] f(-k\tau) \right. \\
&\quad \left. + \xi_*^2 (1 + s_{\theta*}^2 c_{\theta*}^2) [f^2(-k\tau) + g(-k\tau)] \right\}, \tag{64}
\end{aligned}$$

$$\begin{aligned}
\bar{\mathcal{C}}_{\mathcal{RS}} &= \left( \frac{H_*^2}{2\pi\dot{\sigma}_*} \right)^2 (1+k^2\tau^2)(1-2\epsilon_*) \left\{ -\frac{\sin(2\Psi_*) + \sin(2\Theta_*)}{2\cos^2(\Theta_* + \Psi_*)} - \frac{(3\lambda_1 - \lambda_1^2)\sin(2\Psi_*) + (3\lambda_2 - \lambda_2^2)\sin(2\Theta_*)}{3\cos^2(\Theta_* + \Psi_*)} f(-k\tau) \right. \\
&\quad - \frac{\lambda_1^2\sin(2\Psi_*) + \lambda_2^2\sin(2\Theta_*)}{2\cos^2(\Theta_* + \Psi_*)} [f(-k\tau)^2 + g(-k\tau)] \\
&\quad + \frac{e^{i\pi(\mu_1-\mu_2)/2}\sin\Psi_*\sin\Theta_* + e^{-i\pi(\mu_1-\mu_2)/2}\cos\Psi_*\cos\Theta_*}{\cos^2(\Theta_* + \Psi_*)} \sin(\Theta_* + \Psi_*) \left[ 1 + \left( \lambda_1 + \lambda_2 - \frac{\lambda_1^2}{3} - \frac{\lambda_2^2}{3} \right) f(-k\tau) \right. \\
&\quad \left. + \lambda_1\lambda_2 f^2(-k\tau) + \frac{1}{2}(\lambda_1^2 + \lambda_2^2) g(-k\tau) \right] \left. \right\} \\
&= \left( \frac{H_*^2}{2\pi\dot{\sigma}_*} \right)^2 (1+k^2\tau^2) \left\{ \left[ 2\xi_* s_{\theta*}^3 - 2\eta_{\sigma s*} - \frac{2}{3}\xi_*^2 c_{\theta*} s_{\theta*}^3 (1 + c_{\theta*}^2) \right] f(-k\tau) + \xi_*^2 c_{\theta*} s_{\theta*}^3 [f^2(-k\tau) + g(-k\tau)] \right. \\
&\quad \left. + \frac{i\pi}{3}\xi_*^2 c_{\theta*}^3 s_{\theta*}^3 \right\}. \tag{65}
\end{aligned}$$

Here we have used overbars to avoid confusions with the notations in equations (81), (82) and (83). Let us comment the above results. First, one can verify that, we recover the results of [12] if we switch off the terms proportional to  $\xi^2$ . Second, our final expression depends explicitly on  $\tau$  and allows us a precise estimate of the spectra around the time of Hubble crossing. At several e-folds after Hubble crossing, we can safely replace the factor  $(1+k^2\tau^2)$  by 1, and the functions  $f(-k\tau)$ ,  $g(-k\tau)$  by the numbers 0.7296 and 1.4672 respectively. The resulted asymptotic values of spectra will be taken as initial conditions for super-horizon evolution in the next subsection.

Another difference with [12] is that the imaginary part of  $\mathcal{C}_{\mathcal{RS}}$  is nonvanishing here although very small. This will be confirmed by numerical simulations in section IV, see figure 5. We should stress that the imaginary part of  $\mathcal{C}_{\mathcal{RS}}$  is of  $\mathcal{O}(\xi^2)$  and thus negligible in the  $\mathcal{O}(\xi)$  analysis.

#### D. Super-horizon evolution

In the previous subsection, we have studied the evolution of perturbations from the sub-horizon scale to several e-folds after Hubble crossing. In this subsection, taking the asymptotic values of (63), (64), (65) as initial conditions, we will study the

evolution of perturbations on the super-horizon scales  $k^2\tau^2 \ll 0$ .

As preparation, it is interesting to note that  $Q_\sigma$  and its time derivative in equation (24) can be eliminated simultaneously with the help of (22), resulting in

$$\ddot{\delta s} + 3H\dot{\delta s} + \left(\frac{k^2}{a^2} + C_{ss} + \frac{4V_s^2}{\dot{\sigma}^2}\right)\delta s + \frac{4M_P^2 V_s}{\dot{\sigma}^2} \frac{k^2}{a^2} \Phi = 0. \quad (66)$$

More interestingly, in terms of the curvature perturbation  $\mathcal{R}$  and the entropy perturbation  $\mathcal{S}$ , we can translate equations (22) and (66) into

$$\dot{\mathcal{R}} = 2(\dot{\theta} + b_\phi \dot{\sigma} \sin \theta) \mathcal{S} - \frac{2M_P^2 H}{\dot{\sigma}^2} \frac{k^2}{a^2} \Phi, \quad (67)$$

$$\ddot{\mathcal{S}} + \left(3H - \frac{2\dot{H}}{H} + \frac{2\ddot{\sigma}}{\dot{\sigma}}\right) \dot{\mathcal{S}} + \left(\frac{k^2}{a^2} + C_{ss} + \frac{4V_s^2}{\dot{\sigma}^2} + 6\dot{H} - V_{\sigma\sigma} - \frac{2\dot{\sigma}V_\sigma}{M_P^2 H} + \frac{2\dot{H}^2}{H^2}\right) \mathcal{S} + \frac{4M_P^2 H V_s}{\dot{\sigma}^3} \frac{k^2}{a^2} \Phi = 0, \quad (68)$$

where equations (6), (9) have been used. In the large-scale limit  $k^2/(a^2 H^2) \rightarrow 0$ , the  $k^2$ -terms are negligible, then the entropy perturbation evolves independently and works as a source term for the curvature perturbation. Unlike the canonical situation [23], even if the inflation trajectory is straight in field space ( $\dot{\theta} = 0$ ), the curvature perturbation is not conserved in the large-scale limit in the presence of entropy perturbation as long as  $\xi \sin \theta \neq 0$ . This conclusion does not rely on slow-roll conditions, initial conditions and sub-horizon evolution.

For the same reason, we omit  $k^2$ -terms in equations (22) and (66), and write down perturbation equations on the super-Hubble scale

$$\dot{\sigma} \dot{Q}_\sigma + \left(3H + \frac{\dot{H}}{H}\right) \dot{Q}_\sigma + V_\sigma Q_\sigma + 2V_s \delta s = 0, \quad (69)$$

$$\ddot{\delta s} + 3H\dot{\delta s} + \left(C_{ss} + \frac{4V_s^2}{\dot{\sigma}^2}\right) \delta s = 0. \quad (70)$$

Starting from the Hubble-crossing spectra (63), (64), (65), in this section we will analytically evolve perturbations on the super-Hubble scales according to equations (69), (70) to the precision of  $\mathcal{O}(\epsilon, \eta, \xi)$  and  $\mathcal{O}(\xi^2)$ . This method is different from that in references [10, 12, 19, 20] and leads to different results even in the first order of  $\xi$ , see equations (77), (C4) and blue dashed lines in figures 3, 4.

To the first order of  $\xi$ , we can neglect the  $\ddot{\delta s}$  term in equation (70) by virtue of the slow-roll conditions. This approximation is supported by the resulted first-order differential equation

$$\dot{\delta s} + \frac{1}{3H} \left(C_{ss} + \frac{4V_s^2}{\dot{\sigma}^2}\right) \delta s + \mathcal{O}(\xi^2) = 0, \quad (71)$$

which implies  $\dot{\delta s} = \mathcal{O}(\xi)$  because

$$C_{ss} + \frac{4V_s^2}{\dot{\sigma}^2} = H^2 [3\eta_{ss} - 3\xi c_\theta (1 + s_\theta^2) - \xi^2 (1 + s_\theta^4 - 4s_\theta^6)] + \mathcal{O}(\epsilon^2, \eta^2, \xi^3, \epsilon\eta, \epsilon\xi, \eta\xi). \quad (72)$$

From equations (10) and (18), it is easy to see

$$\dot{\theta} = -H (\eta_{\sigma s} + \xi s_\theta c_\theta^2). \quad (73)$$

Differentiating equation (71) with the help of the above equation, we get

$$\ddot{\delta s} + H [\eta_{ss} - \xi c_\theta (1 + s_\theta^2)] \dot{\delta s} + H^2 \xi^2 s_\theta^2 c_\theta^2 (3c_\theta^2 - 2) \delta s + \mathcal{O}(\epsilon^2, \eta^2, \xi^3, \epsilon\eta, \epsilon\xi, \eta\xi) = 0. \quad (74)$$

Now it is clear that  $\ddot{\delta s} = \mathcal{O}(\xi^2)$  as we have expected. We can eliminate the  $\ddot{\delta s}$  term in equations (70) and (74), obtaining

$$H [3 - \eta_{ss} + \xi c_\theta (1 + s_\theta^2)] \dot{\delta s} + H^2 [3\eta_{ss} - 3\xi c_\theta (1 + s_\theta^2) - \xi^2 (1 + s_\theta^2 - 3s_\theta^4 - s_\theta^6)] \delta s + \mathcal{O}(\epsilon^2, \eta^2, \xi^3, \epsilon\eta, \epsilon\xi, \eta\xi) = 0. \quad (75)$$

Neglecting corrections of  $\mathcal{O}(\epsilon^2, \eta^2, \xi^3, \epsilon\eta, \epsilon\xi, \eta\xi)$ , we can write equations (69) and (75) in the form

$$\dot{Q}_\sigma \simeq AHQ_\sigma + BH\delta s, \quad \dot{\delta s} \simeq DH\delta s, \quad (76)$$

where

$$A = 2\epsilon - \eta_{\sigma\sigma}, \quad B = 2\xi s_\theta^3 - 2\eta_{\sigma s}, \quad D = \xi c_\theta(1 + s_\theta^2) - \eta_{ss} - \frac{2}{3}\xi^2 s_\theta^4. \quad (77)$$

Their solutions are

$$Q_\sigma(N) \simeq e^{AN} Q_{\sigma*} + \frac{B}{D-A} (e^{DN+\beta N^2} - e^{AN}) \delta_{s*}, \quad \delta_s(N) \simeq e^{DN+\beta N^2} \delta_{s*}, \quad (78)$$

where

$$\beta = \frac{1}{2}\xi^2 (1 - 3s_\theta^2) s_\theta^2 c_\theta^2. \quad (79)$$

In the slow-roll approximation, we can make use of the background equations to prove the following equation

$$\frac{1}{H} \frac{d}{dt} \ln \frac{H}{\dot{\sigma}} = -2\epsilon + \eta_{\sigma\sigma} \quad (80)$$

which leads to  $H/\dot{\sigma} \simeq (H_*/\dot{\sigma}_*)e^{-AN}$ . Recalling that  $Q_\sigma$  and  $\delta_s$  are related to the curvature and entropy perturbations by (20) and taking the above results into account, we immediately get the power spectra and correlations on super-Hubble scales

$$\mathcal{P}_\mathcal{R}(N) \simeq \mathcal{P}_{\mathcal{R}*} + \mathcal{P}_{\mathcal{S}*} \left( \frac{B}{\gamma} \right)^2 (e^{\gamma N + \beta N^2} - 1)^2 + 2\text{Re}(\mathcal{C}_{\mathcal{R}\mathcal{S}*}) \frac{B}{\gamma} (e^{\gamma N + \beta N^2} - 1), \quad (81)$$

$$\mathcal{C}_{\mathcal{R}\mathcal{S}}(N) \simeq \mathcal{C}_{\mathcal{R}\mathcal{S}*} e^{\gamma N + \beta N^2} + \mathcal{P}_{\mathcal{S}*} \frac{B}{\gamma} e^{\gamma N + \beta N^2} (e^{\gamma N + \beta N^2} - 1), \quad (82)$$

$$\mathcal{P}_\mathcal{S}(N) \simeq \mathcal{P}_{\mathcal{S}*} e^{2\gamma N + 2\beta N^2}, \quad (83)$$

where  $\gamma = D - A$ . In the next subsection, we will regard  $A$ ,  $B$  and  $D$  as constants, i.e. their Hubble-crossing values. What is more,  $\mathcal{P}_{\mathcal{R}*}$ ,  $\mathcal{P}_{\mathcal{S}*}$  and  $\mathcal{C}_{\mathcal{R}\mathcal{S}*}$  can be estimated by the asymptotic values of  $\bar{\mathcal{P}}_\mathcal{R}$ ,  $\bar{\mathcal{P}}_\mathcal{S}$  and  $\bar{\mathcal{C}}_{\mathcal{R}\mathcal{S}}$ , namely by taking the  $k\tau \rightarrow 0$  limit of (63), (64), (65). It is intriguing to note that at large e-folds, equations (81), (82) and (83) are all dominated by a term proportional to  $\mathcal{P}_{\mathcal{S}*}$ . By definition of the relative correlation coefficient (54),  $|\bar{\mathcal{C}}|$  tends to 1 at large  $N$ . This explains the behavior of  $|\bar{\mathcal{C}}|$  in figure 5.

When the entropy perturbation is absent, the curvature perturbation remains frozen on super-Hubble scales as a consequence of equation (67). In this particular situation, the power spectra of curvature perturbation is given by the single-field result

$$\mathcal{P}_\mathcal{R}^{\text{sf}}(k) \simeq \frac{H^2}{4\pi^2 \dot{\sigma}^2}. \quad (84)$$

Its Hubble-crossing value  $\mathcal{P}_{\mathcal{R}*}^{\text{sf}}$  will be utilized to normalize the power spectra and correlations when comparing with numerical examples.

#### IV. COMPARISON WITH NUMERICAL EXAMPLES

In the previous section, we have calculated the power spectra and correlations for curvature and entropy perturbations analytically. Although the details are complicated, the logic is quite clear: we solve the coupled system of differential equations (23) and (24) with the initial conditions (28), and then evaluate the power spectra and correlations according to definitions (53). The same logic can be also applied to numerical calculations. A numerical approach has been developed in reference [19] by virtue that  $e_\sigma$  and  $e_s$  are two independent Gaussian random variables. In this approach, one has to run the integration algorithm twice. In the first run, one sets  $e_s = 0$  in the initial conditions (28) and gets the numerical solutions  $\mathcal{R} = \mathcal{R}_1$  and  $\mathcal{S} = \mathcal{S}_1$ . In the second run, one chooses  $e_\sigma = 0$  and gets  $\mathcal{R} = \mathcal{R}_2$  and  $\mathcal{S} = \mathcal{S}_2$ . Then the power spectra and correlations can be evaluated by [19]

$$\begin{aligned} \mathcal{P}_\mathcal{R} &= \frac{k^3}{2\pi^2} (|\mathcal{R}_1|^2 + |\mathcal{R}_2|^2), \\ \mathcal{P}_\mathcal{S} &= \frac{k^3}{2\pi^2} (|\mathcal{S}_1|^2 + |\mathcal{S}_2|^2), \\ \mathcal{C}_{\mathcal{R}\mathcal{S}} &= \frac{k^3}{2\pi^2} (\mathcal{R}_1^\dagger \mathcal{S}_1 + \mathcal{R}_2^\dagger \mathcal{S}_2). \end{aligned} \quad (85)$$

This numerical method was adopted in reference [12] to judge their analytical results. We will follow it in this paper.

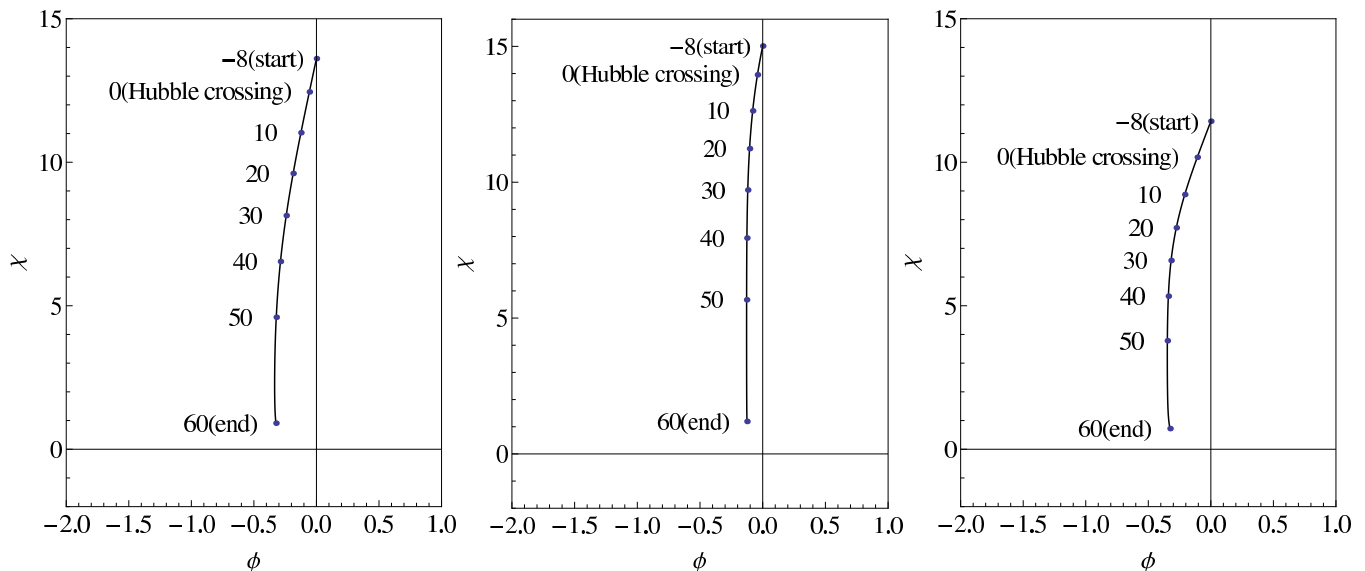


Figure 1. (color online). The classical inflationary trajectory for model (86) with parameters given by (87). At the start point  $N = -8$ ,  $\phi = 0$  as we set. The left panel is the same of figure 1(b) in reference [12].

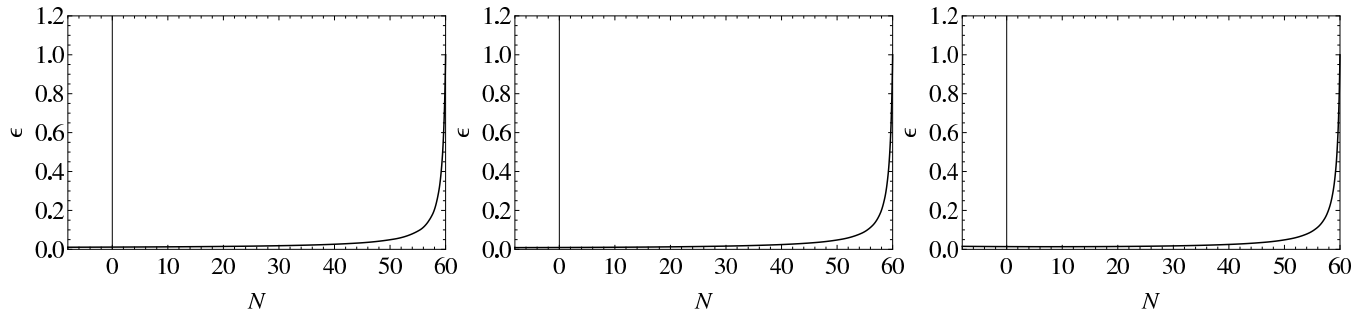


Figure 2. (color online). The evolution of slow-roll parameter  $\epsilon$  in model (86) with parameters given by (87). At the end point  $N = 60$ ,  $\epsilon = 1$  as we set.

As an example, we apply our analytical results and this numerical algorithm to a typical model described by

$$b(\phi) = -\frac{\alpha\phi}{M_P}, \quad V(\phi, \chi) = \frac{1}{2}m_\phi^2\phi^2 + \frac{1}{2}m_\chi^2\chi^2. \quad (86)$$

Concretely, in all figures of this paper, we work out three benchmarks with the following choices of parameters

$$\begin{aligned} \text{Left panels :} & \quad \alpha = 1, \quad m_\phi = m_\chi; \\ \text{Middle panels :} & \quad \alpha = 1, \quad m_\phi = 2m_\chi; \\ \text{Right panels :} & \quad \alpha = \frac{3}{2}, \quad m_\phi = m_\chi. \end{aligned} \quad (87)$$

The left-panel benchmark is exactly the double inflation model with non-canonical kinetic terms in reference [12].

In the slow-roll approximation, the background equations of motion (3) and (4) reduce to a couple of first-order differential equations. Therefore, to numerically solve the background equations, we need two boundary conditions. Following reference [12], our algorithm starts at eight e-folds before the Hubble crossing and ends at 60 e-folds after Hubble crossing. At the start point  $N = -8$ , we set  $\phi = 0$  in accordance with the canonical initial conditions (28). At the end point  $N = 60$ , we set  $\epsilon = 1$  to make sure the slow-roll condition breaks down as the inflation ends.

Figures 1 and 2 correspond to our numerical results of the background evolution. The classical inflationary trajectories in the field space are depicted in figure 1. In every panel of the figure, the field  $\chi$  decreases monotonically, while field  $\phi$  moves from zero to the negative direction and then returns, forming a bent trajectory. The turn point and the exact shape of trajectory are sensitive to model parameters. The evolution of slow-roll parameter  $\epsilon$  is shown in figure 2. In all panels of this figure, we can see  $\epsilon$  has been kept very small until an instant near the end of inflation  $N = 60$ .

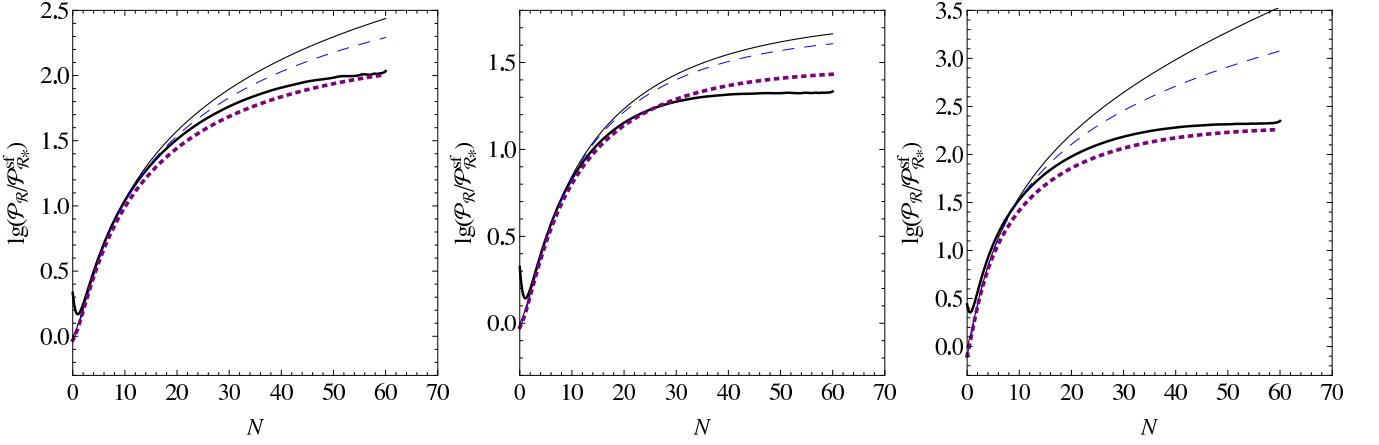


Figure 3. (color online). Three different analytical predictions against the numerical result for the power spectrum of curvature perturbation  $\mathcal{P}_R$  in model (86) with parameters given by (87). Thick solid lines depict the numerical result, and thin solid lines show the analytical prediction of reference [12]. Our analytical predictions (81) are shown by blue dashed lines without  $\xi^2$  terms and purple dotted lines with  $\xi^2$  terms.

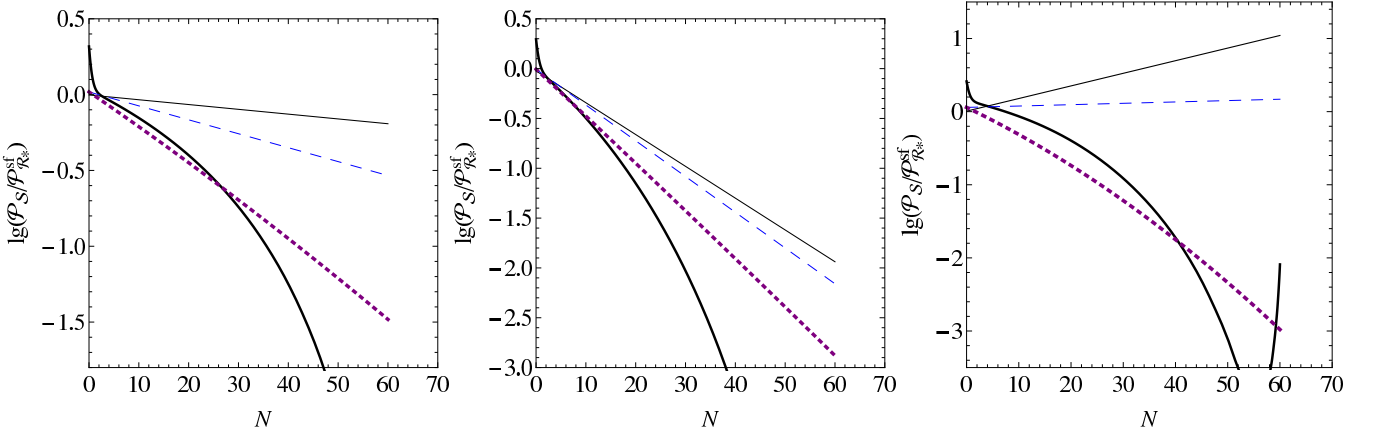


Figure 4. (color online). Three different analytical predictions against the numerical result for the power spectrum of entropy perturbation  $\mathcal{P}_S$  in model (86) with parameters given by (87). Thick solid lines depict the numerical result, and thin solid lines show the analytical prediction of reference [12]. Our analytical predictions (81) are shown by blue dashed lines without  $\xi^2$  terms and purple dotted lines with  $\xi^2$  terms.

Figures 3, 4 and 5 show analytical predictions for the power spectra and the relative correlation coefficient against numerical results. In these figures, thick solid lines depict results from the full numerical approach (85), while thin solid lines reproduce the analytical results of reference [12]. The blue dashed lines show our analytical results (81), (82) and (83) but with  $\mathcal{O}(\xi^2)$  terms switched off, which fit the numerical results better than thin solid lines. The purple dotted lines depict our analytical results (81), (82) and (83) to  $\mathcal{O}(\xi^2)$ , which fit the numerical results best. As we have discussed in subsection III D, our treatment of super-horizon perturbations is different from that in references [10, 12, 19, 20] and leads to different results even in  $\mathcal{O}(\xi)$ . This is demonstrated by the difference between thin solid lines and the blue dashed lines.

In figures 3 and 4, the power spectra  $\mathcal{P}_R$  and  $\mathcal{P}_S$  are normalized to the Hubble-crossing value of (84), namely  $\mathcal{P}_{R*}^{\text{sf}} \simeq H_*^4/4\pi^2\dot{\sigma}_*^2$ . In figure 5, we present the magnitude as well as the imaginary part of the relative correlation coefficient  $\tilde{C}$ . Because  $\text{Im } \tilde{C}$  is of  $\mathcal{O}(\xi^2)$ , there is neither a thin solid line nor a blue dashed line for  $\lg |\text{Im } \tilde{C}|$ . For the same reason, the magnitude of  $\tilde{C}$  is dominated by its real part, and all analytical results coincide with the numerical result. The large- $N$  behavior of  $|\tilde{C}|$  is also in accordance with our analysis below equation (83).

## V. COMMENT

In this paper, we analytically computed the primordial power spectra to the precision of  $\mathcal{O}(\epsilon, \eta, \xi)$  and  $\mathcal{O}(\xi^2)$  for inflation model (1). When doing this, we found the perturbation equations (41) cannot be diagonalized through an orthogonal similarity transformation, because a term of order  $\xi^2$  makes the coefficient matrix (43) nonsymmetric. This difficulty can be overcome

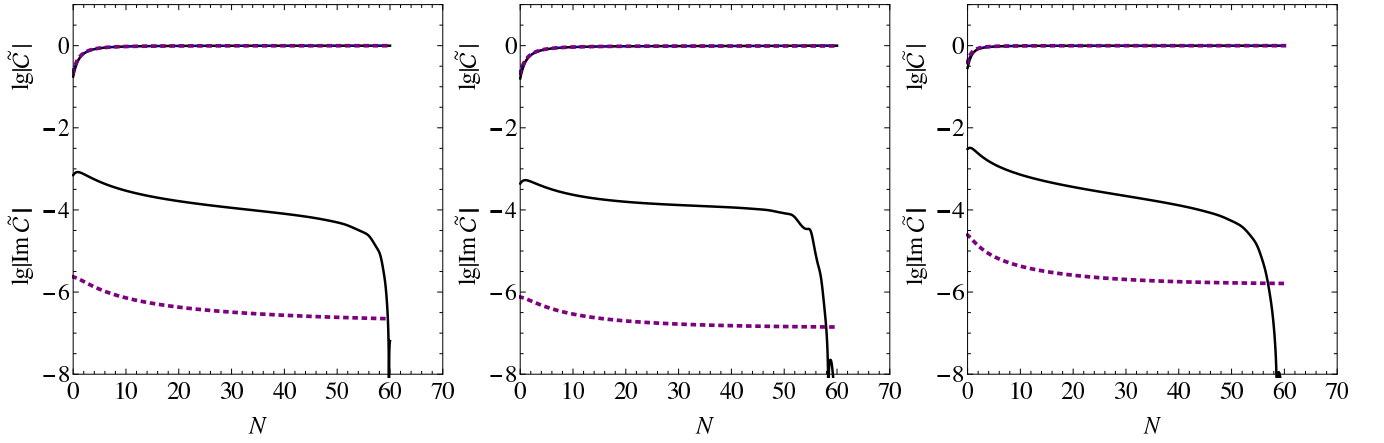


Figure 5. (color online). Three different analytical predictions against the numerical result for the relative correlation coefficient  $\tilde{C}$  in model (86) with parameters given by (87). Thick solid lines depict the numerical result, and thin solid lines show the analytical prediction of reference [12]. Our analytical predictions (81) are shown by blue dashed lines without  $\xi^2$  terms and purple dotted lines with  $\xi^2$  terms. All analytical predictions for  $|\tilde{C}|$  coincide almost perfectly with the numerical result, approaching 1 at large e-folds. Because the imaginary part of  $\mathcal{C}_{\mathcal{R},S}$  is of order  $\xi^2$ , we plot neither a thin solid line nor a blue dashed line for  $\lg |\text{Im } \tilde{C}|$ .

by introducing a nonorthogonal diagonalization (44) and a nonorthogonal basis (31) at Hubble crossing. To keep the  $\mathcal{O}(\xi^2)$  corrections, we expanded the Hankel function (58) to the second order. On the super-horizon scale,  $\ddot{Q}_\sigma$  and  $\ddot{\delta}s$  terms, which were discarded in the past, also bring  $\mathcal{O}(\xi^2)$  corrections to the primordial perturbations. To take them into account, we solved the super-horizon equations by iteration.

Neglecting the  $k^2$ -terms on the super-horizon scale, the evolution of curvature and entropy perturbations can be described by equations (69) and (70), or equivalently by equations (C1) and (70). Only (69) is a first-order differential equation. In references [10, 12, 19, 20], equations (69) and (70) are both truncated from second-order to first-order differential equations to solve super-horizon perturbations analytically. In the main body of this paper, we evolved the perturbations according to equation (69) and the truncated form of (70). Our  $\mathcal{O}(\xi)$  analytical result is different from that of reference [12] and fits the numerical result better. This can be seen by comparing the blue dashed lines with thin solid lines in figures 3 and 4. For these two approaches,  $\mathcal{O}(\xi^2)$  analytical results are derived in subsection III D and appendix C respectively. Again our analytical result fits better, see purple dotted lines in figures 3, 4 and black dotted lines in figure 6.

But this is not the full story. In subsection (III D), we claimed that the background equations lead to  $H/\dot{\sigma} \simeq (H_*/\dot{\sigma}_*)e^{-AN}$  with  $A$  given by equation (77). However, in reference [12], it is mentioned that  $H/\dot{\sigma} \simeq (H_*/\dot{\sigma}_*)e^{-AN}$  and  $A$  is given by equation (C4) without the  $\mathcal{O}(\xi^2)$  term. In drawing the thin solid lines and the black dotted lines, we have set the value of  $A$  according to equation (C4) without and with the  $\mathcal{O}(\xi^2)$  term, respectively. For both blue dashed lines and purple dotted lines,  $A$  was dictated by equation (77). Interestingly, if we choose  $A$  in the expression of  $H/\dot{\sigma}$  according to equation (77), then for  $\mathcal{P}_{\mathcal{R}}$  the thin solid lines will get closer to thick solid lines, but the black dotted lines will deviate away from them. In the meanwhile, for  $\mathcal{P}_{\mathcal{S}}$  and  $\mathcal{C}_{\mathcal{R},S}$ , the thin solid lines will coincide with blue dashed lines, and the black dotted lines will coincide with purple dotted lines.

## ACKNOWLEDGMENTS

This work is supported by the National Natural Science Foundation of China (Grant Nos. 11105053 and 91536218).

## Appendix A: Diagonalization of $\tilde{\mathbf{M}}$

If  $(a-d)^2 + 4bc > 0$ , an arbitrary matrix of two dimensions

$$\tilde{\mathbf{M}} = \begin{pmatrix} a & b \\ c & d \end{pmatrix} \quad (\text{A1})$$

can be always diagonalized by transformation (44) with  $\tilde{\mathbf{R}}_*^{-1}$  given by (45) and

$$\begin{aligned}\tilde{\lambda}_1 &= \frac{1}{2} \left[ a + d - \sqrt{(a-d)^2 + 4bc} \right], \\ \tilde{\lambda}_2 &= \frac{1}{2} \left[ a + d + \sqrt{(a-d)^2 + 4bc} \right].\end{aligned}\quad (\text{A2})$$

Specifically, when  $\tilde{\mathbf{M}}$  takes the form (43) with  $\xi < 0$ , its eigenvalues are

$$\begin{aligned}\tilde{\lambda}_1 &\simeq (1 + 3s_\theta^2)^{-1/2} \left[ \xi^2 \left( \frac{3}{2}c_\theta^5 - 4c_\theta^3 + 3c_\theta \right) - 6\eta_{\sigma s}s_\theta^3 + \left( \frac{3}{2}\eta_{ss} - \frac{3}{2}\eta_{\sigma\sigma} + 3\epsilon \right) (2c_\theta^3 - 3c_\theta) \right] \\ &\quad + \frac{3}{2}\xi \left( \sqrt{1 + 3s_\theta^2} - c_\theta \right) + \frac{3}{2}\eta_{ss} + \frac{3}{2}\eta_{\sigma\sigma} + \frac{1}{2}\xi^2 s_\theta^4 - \frac{1}{2}\xi^2 - 3\epsilon + \mathcal{O}(\epsilon^2, \eta^2, \xi^3, \epsilon\eta, \epsilon\xi, \eta\xi), \\ \tilde{\lambda}_2 &\simeq -(1 + 3s_\theta^2)^{-1/2} \left[ \xi^2 \left( \frac{3}{2}c_\theta^5 - 4c_\theta^3 + 3c_\theta \right) - 6\eta_{\sigma s}s_\theta^3 + \left( \frac{3}{2}\eta_{ss} - \frac{3}{2}\eta_{\sigma\sigma} + 3\epsilon \right) (2c_\theta^3 - 3c_\theta) \right] \\ &\quad - \frac{3}{2}\xi \left( \sqrt{1 + 3s_\theta^2} + c_\theta \right) + \frac{3}{2}\eta_{ss} + \frac{3}{2}\eta_{\sigma\sigma} + \frac{1}{2}\xi^2 s_\theta^4 - \frac{1}{2}\xi^2 - 3\epsilon + \mathcal{O}(\epsilon^2, \eta^2, \xi^3, \epsilon\eta, \epsilon\xi, \eta\xi),\end{aligned}\quad (\text{A3})$$

and one obtains the following combinations useful for deriving equations (63), (64) and (65),

$$\begin{aligned}\tan(\Theta + \Psi) &= \frac{2\xi s_\theta^3 c_\theta^3}{3\sqrt{1 + 3s_\theta^2}} + \mathcal{O}(\epsilon, \eta, \xi^2), \\ \frac{\cos(\Theta - \Psi)}{\cos(\Theta + \Psi)} &= -\frac{2c_\theta^3 - 3c_\theta}{\sqrt{1 + 3s_\theta^2}} - \frac{4s_\theta^3 [\eta_{\sigma s} (6c_\theta^3 - 9c_\theta) + s_\theta^3 (3\eta_{ss} - 3\eta_{\sigma\sigma} - 2\xi^2 + 6\epsilon)]}{3\xi (1 + 3s_\theta^2)^{3/2}} + \mathcal{O}(\epsilon, \eta, \xi^2), \\ \frac{\sin(\Theta - \Psi)}{\cos(\Theta + \Psi)} &= -\frac{2s_\theta^3}{\sqrt{1 + 3s_\theta^2}} + \frac{(4c_\theta^3 - 6c_\theta) [\eta_{\sigma s} (6c_\theta^3 - 9c_\theta) + s_\theta^3 (3\eta_{ss} - 3\eta_{\sigma\sigma} - 2\xi^2 + 6\epsilon)]}{3\xi (1 + 3s_\theta^2)^{3/2}} + \mathcal{O}(\epsilon, \eta, \xi^2).\end{aligned}\quad (\text{A4})$$

### Appendix B: Expansion of the Hankel function

In terms of the gamma function  $\Gamma(\mu)$  and Bessel functions of the first kind  $J_\mu(x)$ , the Hankel function  $H_\mu^{(1)}(x)$  can be expressed as equations (56) and expanded as

$$\begin{aligned}H_\mu^{(1)}(x) &= \frac{J_{-\mu}(x) - e^{-i\mu\pi} J_\mu(x)}{i \sin(\mu\pi)} \\ &= \frac{1}{i \sin(\mu\pi)} \left[ \sum_{m=0}^{\infty} \frac{(-1)^m}{m! \Gamma(m - \mu + 1)} \left(\frac{x}{2}\right)^{2m - \mu} - \sum_{m=0}^{\infty} \frac{(-1)^m}{m! \Gamma(m + \mu + 1)} \left(\frac{x}{2}\right)^{2m + \mu} e^{-i\mu\pi} \right] \\ &\simeq \frac{1}{i \sin(\mu\pi)} \left(\frac{2}{x}\right)^\mu \left[ \frac{1}{\Gamma(1 - \mu)} - \frac{1}{\Gamma(2 - \mu)} \left(\frac{x}{2}\right)^2 \right] \\ &= \frac{1}{i\pi} \left(\frac{2}{x}\right)^\mu \Gamma(\mu) \left[ 1 - \frac{\Gamma(1 - \mu)}{\Gamma(2 - \mu)} \left(\frac{x}{2}\right)^2 \right] \\ &= \frac{1}{i\pi} \left(\frac{2}{x}\right)^\mu \Gamma(\mu) \left[ 1 - \frac{1}{1 - \mu} \left(\frac{x}{2}\right)^2 \right]\end{aligned}\quad (\text{B1})$$

for  $\mu \simeq 3/2$  and  $x \ll 1$ , where we have made use of the equality

$$\frac{\pi}{\sin(\mu\pi)} = \Gamma(\mu)\Gamma(1 - \mu).\quad (\text{B2})$$

Apparently, when  $x \rightarrow 0$ , the Hankel function  $H_\mu^{(1)}(x)$  is divergent as  $x^{-\mu}$ . In this paper, we renormalize  $H_\mu^{(1)}(x)$  as

$$\tilde{H}_\mu^{(1)}(x) \equiv x^\mu H_\mu^{(1)}(x)\quad (\text{B3})$$

and define

$$f(x) = \frac{1}{\tilde{H}_{3/2}^{(1)}(x)} \frac{d\tilde{H}_\mu^{(1)}(x)}{d\mu} \Big|_{\mu=3/2}, \quad g(x) = \frac{1}{\tilde{H}_{3/2}^{(1)}(x)} \frac{d^2\tilde{H}_\mu^{(1)}(x)}{d\mu^2} \Big|_{\mu=3/2}.\quad (\text{B4})$$

Then  $\tilde{H}_{\mu A}^{(1)}(x)$  can be expanded to  $\mathcal{O}(\lambda_A^2)$  as (58).

With the help of polygamma function, we can get the numerical values of  $f(x)$  and  $g(x)$ . The polygamma function of order  $m$  is defined as

$$\psi^{(m)}(x) \equiv \frac{d^{m+1}}{dx^{m+1}} \ln \Gamma(x), \quad (\text{B5})$$

which can be calculated by the integrations

$$\psi^{(0)}(x) = -\gamma + \int_0^1 \frac{1-t^{x-1}}{1-t} dt, \quad \psi^{(m)}(x) = -\int_0^1 \frac{t^{x-1}}{1-t} \ln^m t dt \quad (\text{B6})$$

if  $x > 0$  and  $m > 0$ . From these formulae, we can derive

$$\psi^{(0)}\left(\frac{3}{2}\right) = 2 - 2 \ln 2 - \gamma, \quad \psi^{(1)}\left(\frac{3}{2}\right) = \frac{\pi^2}{2} - 4. \quad (\text{B7})$$

Using the above definitions and equations, we can compute  $f(x)$  and  $g(x)$  to  $\mathcal{O}(x^2)$  as

$$\begin{aligned} f(x) &= \left. \frac{d \ln \tilde{H}_\mu^{(1)}(x)}{d\mu} \right|_{\mu=3/2} \\ &= \ln 2 + \left. \frac{d \ln \Gamma(x)}{d\mu} \right|_{\mu=3/2} - \frac{1}{(1-\mu)^2} \left(\frac{x}{2}\right)^2 \left[1 - \frac{1}{1-\mu} \left(\frac{x}{2}\right)^2\right]^{-1} \Big|_{\mu=3/2} \\ &= \ln 2 + \psi^{(0)}\left(\frac{3}{2}\right) - x^2 \left(1 + \frac{x^2}{2}\right)^{-1} \\ &= 2 - \ln 2 - \gamma - \frac{2x^2}{2+x^2} \\ &= 0.7296 - x^2 + \mathcal{O}(x^4), \end{aligned} \quad (\text{B8})$$

$$\begin{aligned} g(x) &= \left[ \left. \frac{d \ln \tilde{H}_\mu^{(1)}(x)}{d\mu} \right]^2 \Big|_{\mu=3/2} + \left. \frac{d^2 \ln \tilde{H}_\mu^{(1)}(x)}{d\mu^2} \right|_{\mu=3/2} \\ &= f^2(x) + \left. \frac{d^2 \ln \Gamma(x)}{d\mu^2} \right|_{\mu=3/2} - \frac{2}{(1-\mu)^3} \left(\frac{x}{2}\right)^2 \left[1 - \frac{1}{1-\mu} \left(\frac{x}{2}\right)^2\right]^{-1} \Big|_{\mu=3/2} \\ &\quad - \frac{1}{(1-\mu)^4} \left(\frac{x}{2}\right)^4 \left[1 - \frac{1}{1-\mu} \left(\frac{x}{2}\right)^2\right]^{-2} \Big|_{\mu=3/2} \\ &= f^2(x) + \psi^{(1)}\left(\frac{3}{2}\right) + 4x^2 \left(1 + \frac{x^2}{2}\right)^{-1} - x^4 \left(1 + \frac{x^2}{2}\right)^{-2} \\ &= \left(2 - \ln 2 - \gamma - \frac{2x^2}{2+x^2}\right)^2 + \frac{\pi^2}{2} - 4 + \frac{8x^2}{2+x^2} - \frac{4x^4}{(2+x^2)^2} \\ &= \frac{\pi^2}{2} + (\ln 2 + \gamma) \left(-4 + \ln 2 + \gamma + \frac{4x^2}{2+x^2}\right) \\ &= 1.4672 + 2.5407x^2 + \mathcal{O}(x^4). \end{aligned} \quad (\text{B9})$$

### Appendix C: $\mathcal{O}(\xi^2)$ corrections to the old routine of super-horizon evolution

The perturbations  $Q_\sigma$  and  $\delta s$  are subject to three differential equations: the constraint (22), which is a first-order differential equation, and the equations of motion (23), (24) which are second-order differential equations. Eliminating  $Q_\sigma$  and  $\dot{Q}_\sigma$  in equation (24) with (22), one can obtain the second-order differential equation (66) for  $\delta s$ . On the super-Hubble scale  $k/(aH) \ll 1$ , the  $k^2$ -terms can be omitted in these equations. In references [10, 12, 19, 20], the super-horizon perturbations are studied

with equations (23) and (66), or more concretely, by truncating the  $\ddot{Q}_\sigma$  term in equation (23) and  $\ddot{\delta}s$  in equation (66). In the main body of this paper, a different approach has been taken: we study the super-horizon perturbations with equation (22) and the truncated form of equation (66). Unlike the second-order differential equation (23), equation (22) is a first-order differential equation and hence can be employed without truncation.

As we have demonstrated in subsection III D,  $\dot{\delta}s = \mathcal{O}(\xi^2)$ . Consequently, to the precision of  $\mathcal{O}(\xi)$ , it is enough for us to discard the  $\dot{\delta}s$  term in equation (66). However, to the precision of  $\mathcal{O}(\xi^2)$ , the  $\dot{\delta}s$  term cannot be naively discarded in equation (66), and the truncation of equation (66) to a first-order equation becomes tricky technically. This has been accomplished in subsection III D.

In this appendix, we intend to incorporate  $\mathcal{O}(\xi^2)$  corrections into the old routine of references [10, 12, 19, 20]. In subsection III D, we have already got the first-order differential equation (75) for  $\delta s$  by neglecting corrections of  $\mathcal{O}(\epsilon^2, \eta^2, \xi^3, \epsilon\eta, \epsilon\xi, \eta\xi)$  in (66). Our task here is to apply the same techniques to equation (23) and get the first-order differential equation for  $Q_\sigma$  with  $\mathcal{O}(\xi^2)$  corrections.

In the large-scale limit  $k^2/(a^2H^2) \rightarrow 0$ , equation (23) reduces to

$$\ddot{Q}_\sigma + 3H\dot{Q}_\sigma + C_{\sigma\sigma}Q_\sigma + \frac{2V_s}{\dot{\sigma}}\dot{\delta}s + C_{\sigma s}\delta s = 0. \quad (C1)$$

Neglecting terms of  $\mathcal{O}(\epsilon, \eta, \xi^2)$ , we can rewrite this equation approximately as

$$\dot{Q}_\sigma + H\xi c_\theta s_\theta^2 Q_\sigma - \frac{2}{3}\xi s_\theta^3 \dot{\delta}s - 2H\xi s_\theta^3 \delta s + \mathcal{O}(\xi^2) = 0. \quad (C2)$$

where we have assumed that  $\ddot{Q}_\sigma = \mathcal{O}(\xi^2)$ . We mention in passing that keeping the  $\mathcal{O}(\epsilon, \eta)$  terms in (C2) does not change our final results. The subsequent calculation will be facilitated if one notes further that the  $\dot{\delta}s$  term is suppressed by a factor  $\xi$  in equation (C2). Differentiating equation (C2) with the help of the (73) and eliminating  $\ddot{Q}_\sigma$ ,  $\dot{\delta}s$  and  $\delta s$  with equations (74) (75) (C1), we get finally

$$H(3 - \xi c_\theta s_\theta^2)\dot{Q}_\sigma + H^2 [3\xi c_\theta s_\theta^2 - 6\epsilon + 3\eta_{\sigma\sigma} + \xi^2 c_\theta^2 s_\theta^2 (1 + c_\theta^2)] Q_\sigma + H^2 (-6\xi s_\theta^3 + 6\eta_{\sigma s} - 4\xi^2 c_\theta^3 s_\theta^3)\delta s + \mathcal{O}(\epsilon^2, \eta^2, \xi^3, \epsilon\eta, \epsilon\xi, \eta\xi) = 0. \quad (C3)$$

Neglecting corrections of  $\mathcal{O}(\epsilon^2, \eta^2, \xi^3, \epsilon\eta, \epsilon\xi, \eta\xi)$ , we can write equations (75) and (C3) in the form (76) with coefficients given by

$$A = -\xi c_\theta s_\theta^2 + 2\epsilon - \eta_{\sigma\sigma} - \frac{2}{3}\xi^2 c_\theta^2 s_\theta^2, \quad B = 2\xi s_\theta^3 - 2\eta_{\sigma s} + \frac{2}{3}\xi^2 c_\theta s_\theta^3 (1 + c_\theta^2), \quad D = \xi c_\theta (1 + s_\theta^2) - \eta_{ss} - \frac{2}{3}\xi^2 s_\theta^4. \quad (C4)$$

It is easy to recover the results of [12] by switching off the terms proportional to  $\xi^2$ . Note the value of  $A$  is different from that in (77) even in  $\mathcal{O}(\xi)$ .

If we take  $H/\dot{\sigma} \simeq (H_*/\dot{\sigma}_*)e^{-AN}$  similar to reference [12], then the power spectra and correlations on super-Hubble scales are the same as (81), (82) and (83), but with  $A$ ,  $B$  and  $D$  given by equations (C4). For this analytical result of  $\mathcal{O}(\xi^2)$ , the power spectra  $\mathcal{P}_\mathcal{R}$ ,  $\mathcal{P}_\mathcal{S}$  and the relative correlation coefficient  $\tilde{C}$  are depicted by black dotted lines in figure 6. Confronted with the numerical result, which is plotted by thick solid lines, this result behaves better than the  $\mathcal{O}(\xi)$  result in [12] as shown by thin solid lines. We recommend section V for more information.

- 
- [1] A. H. Guth, Phys. Rev. D **23**, 347 (1981).
  - [2] Q. G. Huang, K. Wang and S. Wang, arXiv:1512.07769 [astro-ph.CO].
  - [3] A. D. Linde, Phys. Lett. B **108**, 389 (1982).
  - [4] A. Albrecht and P. J. Steinhardt, Phys. Rev. Lett. **48**, 1220 (1982).
  - [5] A. A. Starobinsky, Phys. Lett. B **91**, 99 (1980).
  - [6] A. Kehagias, A. M. Dizgah and A. Riotto, Phys. Rev. D **89**, no. 4, 043527 (2014) [arXiv:1312.1155 [hep-th]].
  - [7] D. Polarski and A. A. Starobinsky, Nucl. Phys. B **385**, 623 (1992).
  - [8] J. Garcia-Bellido and D. Wands, Phys. Rev. D **53**, 5437 (1996) [astro-ph/9511029].
  - [9] D. Langlois, Phys. Rev. D **59**, 123512 (1999) [astro-ph/9906080].
  - [10] F. Di Marco and F. Finelli, Phys. Rev. D **71**, 123502 (2005) [astro-ph/0505198].
  - [11] K. Y. Choi, L. M. H. Hall and C. van de Bruck, JCAP **0702**, 029 (2007) [astro-ph/0701247].
  - [12] Z. Lalak, D. Langlois, S. Pokorski and K. Turzyski, JCAP **0707**, 014 (2007) [arXiv:0704.0212 [hep-th]].
  - [13] C. M. Peterson and M. Tegmark, Phys. Rev. D **83**, 023522 (2011) [arXiv:1005.4056 [astro-ph.CO]].

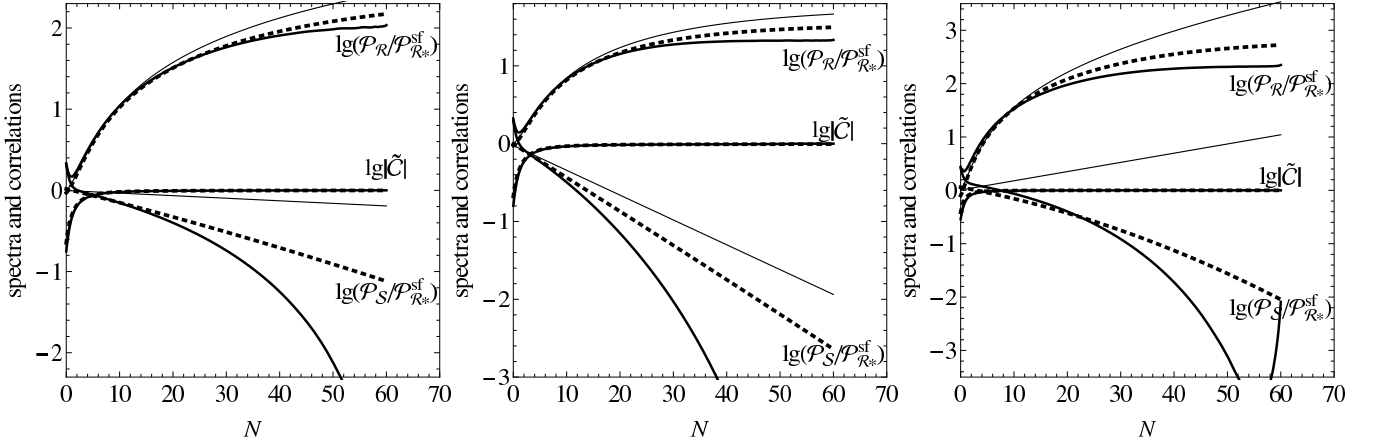


Figure 6. (color online). Two different analytical predictions against the numerical result for the power spectra  $\mathcal{P}_R$ ,  $\mathcal{P}_S$  and the relative correlation coefficient  $\tilde{\mathcal{C}}$  in model (86) with parameters given by (87). Thick solid lines depict the numerical result, and thin solid lines show the analytical prediction of reference [12]. Black dotted lines are drawn by incorporating  $\mathcal{O}(\xi^2)$  corrections into the old routine of references [10, 12, 19, 20].

- [14] K. i. Maeda, Phys. Rev. D **39**, 3159 (1989).
- [15] S. Nojiri and S. D. Odintsov, Phys. Rev. D **68**, 123512 (2003) doi:10.1103/PhysRevD.68.123512 [hep-th/0307288].
- [16] J. c. Hwang and H. Noh, Phys. Rev. D **71**, 063536 (2005) [gr-qc/0412126].
- [17] X. d. Ji and T. Wang, Phys. Rev. D **79**, 103525 (2009) [arXiv:0903.0379 [hep-th]].
- [18] N. Tamanini and C. G. Boehmer, Phys. Rev. D **87**, no. 8, 084031 (2013) doi:10.1103/PhysRevD.87.084031 [arXiv:1302.2355 [gr-qc]].
- [19] S. Tsujikawa, D. Parkinson and B. A. Bassett, Phys. Rev. D **67**, 083516 (2003) [astro-ph/0210322].
- [20] N. Bartolo, S. Matarrese and A. Riotto, Phys. Rev. D **64**, 123504 (2001) [astro-ph/0107502].
- [21] C. Gordon, D. Wands, B. A. Bassett and R. Maartens, Phys. Rev. D **63**, 023506 (2001) [astro-ph/0009131].
- [22] C. T. Byrnes and D. Wands, Phys. Rev. D **74**, 043529 (2006) [astro-ph/0605679].
- [23] D. Wands, Lect. Notes Phys. **738**, 275 (2008) [astro-ph/0702187 [ASTRO-PH]].